

Research Article

Approximate Analysis of MHD Squeeze Flow between Two Parallel Disks with Suction or Injection by Homotopy Perturbation Method

G. Domairry¹ and A. Aziz²

¹ *Department of Mechanical Engineering, Babol University of Technology, P.O. Box 484, Babol, Iran*

² *Department of Mechanical Engineering, School of Engineering & Applied Science, Gonzaga University, Spokane, WA 99268, USA*

Correspondence should be addressed to A. Aziz, aziz@gonzaga.edu

Received 26 January 2009; Accepted 24 March 2009

Recommended by Ji Huan He

An analysis has been performed to study magneto-hydrodynamic (MHD) squeeze flow between two parallel infinite disks where one disk is impermeable and the other is porous with either suction or injection of the fluid. We investigate the combined effect of inertia, electromagnetic forces, and suction or injection. With the introduction of a similarity transformation, the continuity and momentum equations governing the squeeze flow are reduced to a single, nonlinear, ordinary differential equation. An approximate solution of the equation subject to the appropriate boundary conditions is derived using the homotopy perturbation method (HPM) and compared with the direct numerical solution (NS). Results showing the effect of squeeze Reynolds number, Hartmann number and the suction/injection parameter on the axial and radial velocity distributions are presented and discussed. The approximate solution is found to be highly accurate for the ranges of parameters investigated. Because of its simplicity, versatility and high accuracy, the method can be applied to study linear and nonlinear boundary value problems arising in other engineering applications.

Copyright © 2009 G. Domairry and A. Aziz. This is an open access article distributed under the Creative Commons Attribution License, which permits unrestricted use, distribution, and reproduction in any medium, provided the original work is properly cited.

1. Introduction

This paper deals with the study of magneto-hydrodynamic (MHD) squeeze flow of an electrically conducting fluid between two infinite, parallel disks. The lower disk is stationary and permeable with (suction or injection). The upper disk is impermeable and moves toward the lower disk with a specified time dependent velocity. The use of a MHD fluid in lubrication prevents the adverse impact of temperature on the fluid viscosity when the system operates under extreme conditions. The problem considered is of general interest in the theory of magneto-hydrodynamic lubrication and other related applications. In particular,

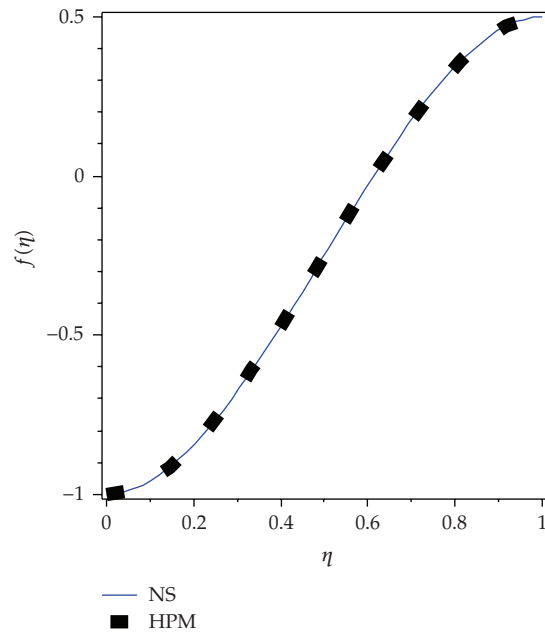


Figure 1: Variation of axial velocity for $M = 0$, $S = 0.01$, $A = -1$.

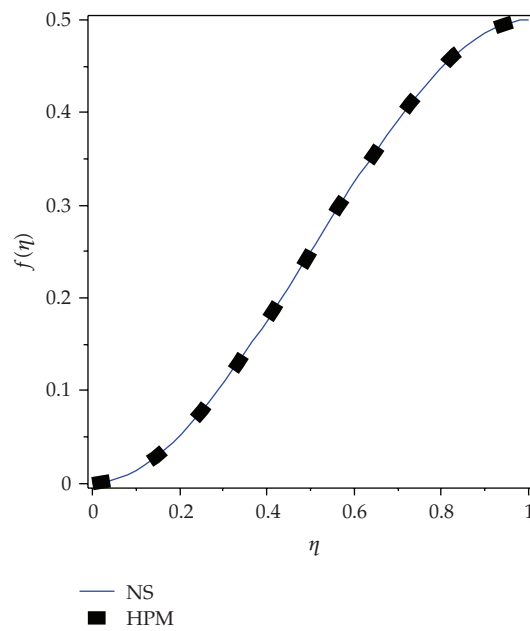


Figure 2: Variation of axial velocity for $M = 0$, $S = 0.01$, $A = 0$.

the results of the present investigation are directly applicable to the hydrodynamics of high temperature bearings lubricated with liquid metals. A number of theoretical and experimental investigations into magneto-hydrodynamic effects in lubrication have been

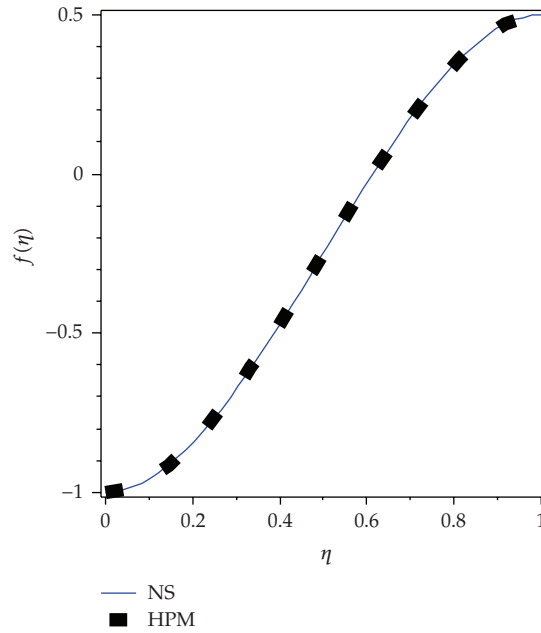


Figure 3: $M = 0, S = 1, A = -1$.

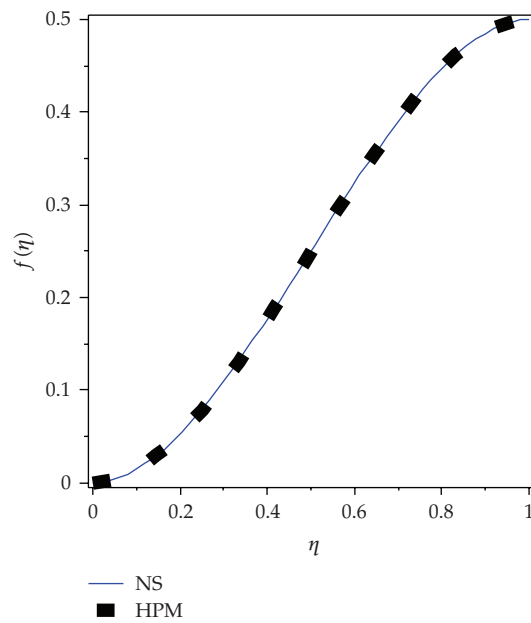


Figure 4: $M = 0, S = 1, A = 0$.

reported. These include among other works of Hughes and Elco [1], Kuzma et al. [2] and Krieger et al. [3]. These authors considered the electromagnetic force term in the Navier-Stokes equations but neglected some or all the inertia terms. When low viscosity lubricants are used to reduce energy losses in lubrication devices, inertial effects become important and must be included especially if the squeeze Reynolds number is not small.

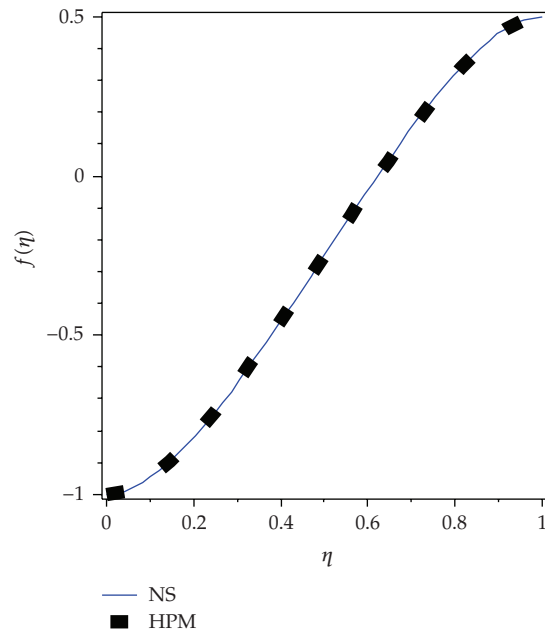


Figure 5: Variation of axial velocity for $M = 5$, $S = 0.01$, $A = -1$.

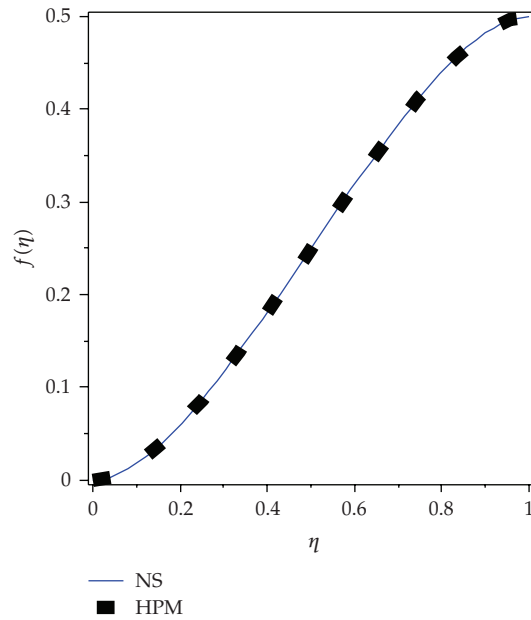


Figure 6: Variation of axial velocity for $M = 5$, $S = 0.01$, $A = 0$.

In the present work we investigate the combined effect of inertia, electromagnetic forces, and surface suction or injection in a squeeze film between two parallel disks. This combination of effects in squeezing flow has not been studied previously. The plates are

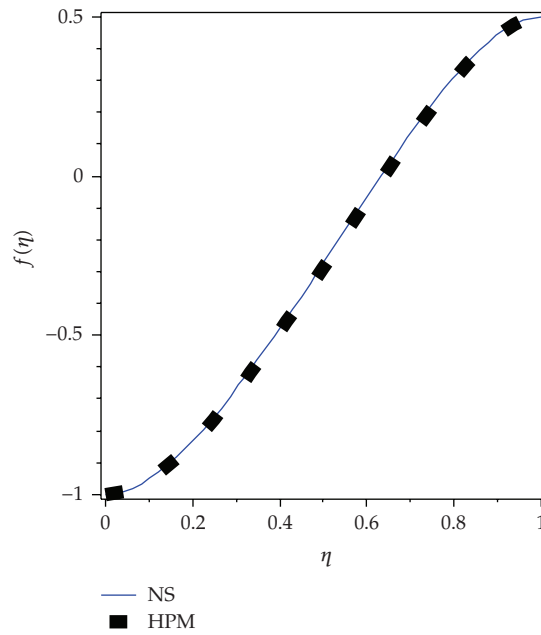


Figure 7: Variation of axial velocity for $M = 5, S = 1, A = -1$.

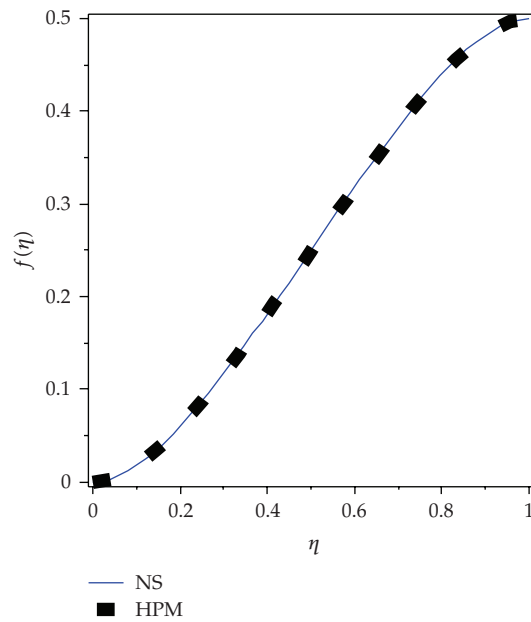


Figure 8: Variation of axial velocity for $M = 5, S = 1, A = 0$.

made of a nonconducting material. There is no externally applied electric field and the induced electric field is negligible. Since the problem defies an exact analytical solution, special techniques must be used to derive approximate analytical solution.

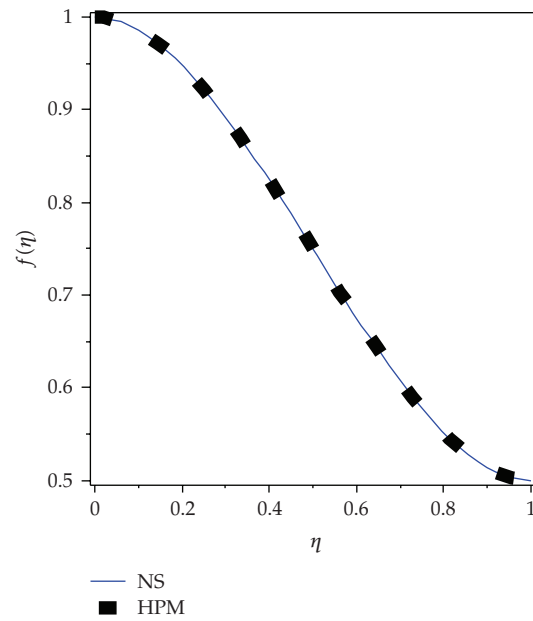


Figure 9: Variation of axial velocity for $M = 0, S = 0.01, A = 1$.

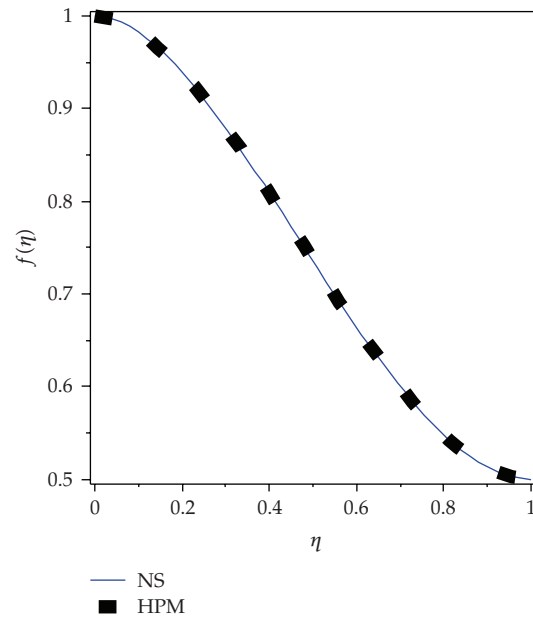


Figure 10: Variation of axial velocity for $M = 0, S = 1, A = 1$.

One such technique is the homotopy perturbation method (HPM) proposed and applied by He [4–6]. His pioneering work has prompted many authors [7–20] to apply HPM to solve a wide variety of homogeneous and nonhomogeneous linear and nonlinear

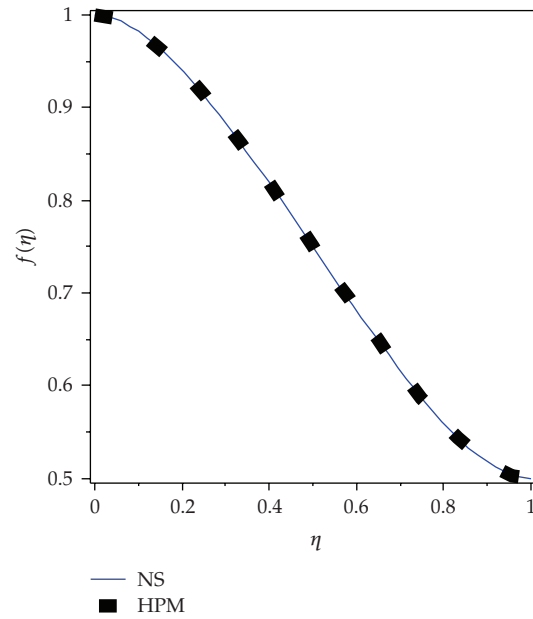


Figure 11: Variation of axial velocity for $M = 5, S = 0.01, A = 1$.

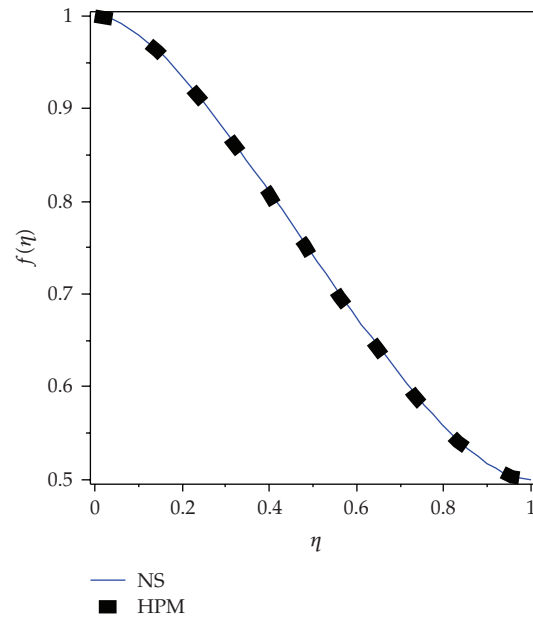


Figure 12: Variation of axial velocity for $M = 5, S = 1, A = 1$.

problems. Over the past several years the accuracy of HPM has been repeatedly verified. In view of the success of HPM reported by many researchers, we were tempted to adopt this method to solve the present problem.

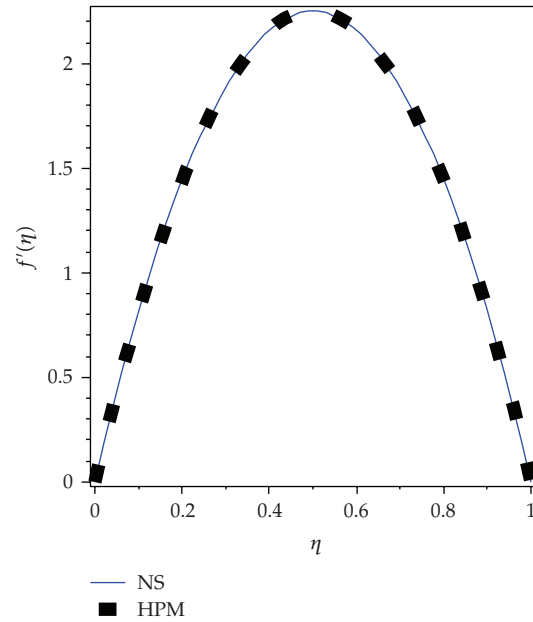


Figure 13: Variation of radial velocity for $M = 0, S = 0.01, A = -1$.

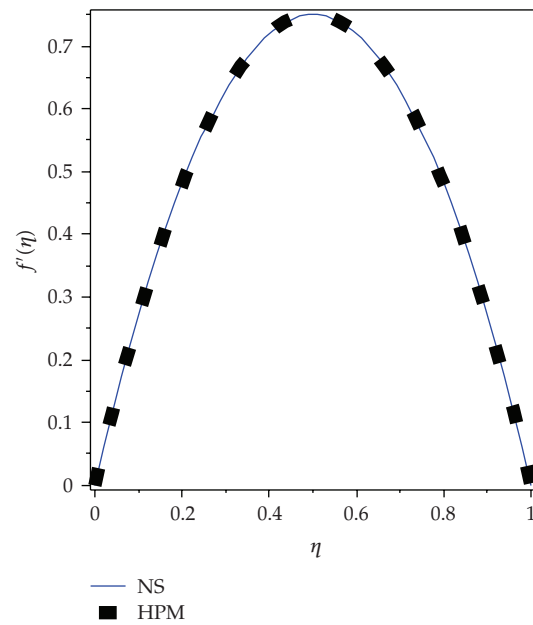


Figure 14: Variation of radial velocity for $M = 0, S = 0.01, A = 0$.

2. The Homotopy Perturbation Method

The basic idea embodied in the HPM and a brief summary of the method can be found in [4-6]. The convergence and stability of this method have been established in [10]. The latest

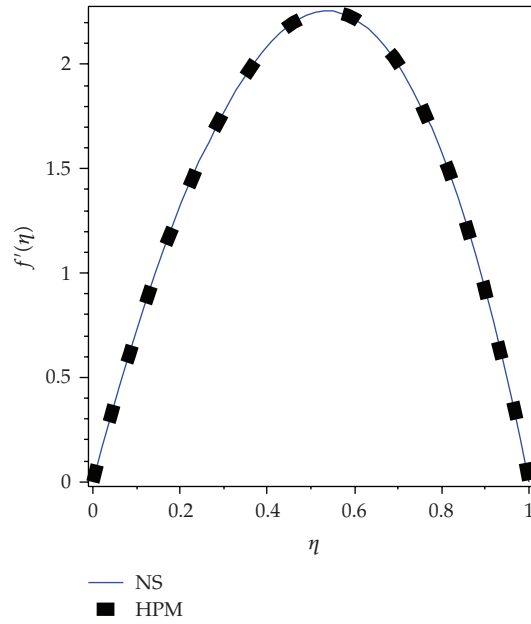


Figure 15: Variation of radial velocity for $M = 0, S = 1, A = -1$.

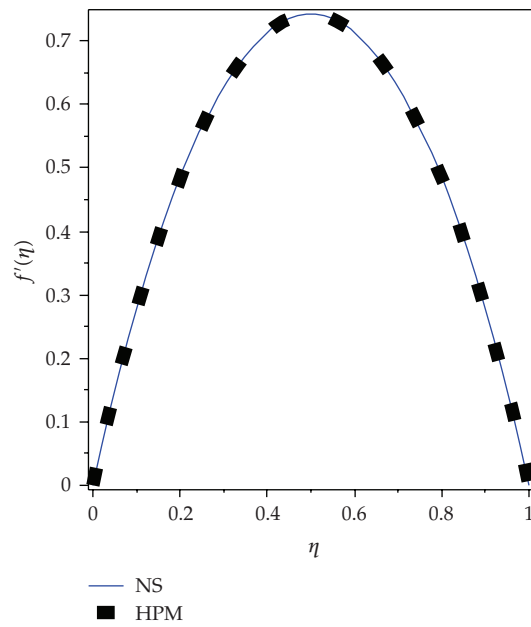


Figure 16: Variation of radial velocity for $M = 0, S = 1, A = 0$.

developments of the method can be found in a series of papers by pioneering researchers such as He [21–23] and Yıldırım [24–30]. Other papers that bear close relevance to the present work are those of Mahmood et al. [31], Mehmood and Ali [32], and Z. Z. Ganji and D. D. Ganji [33].

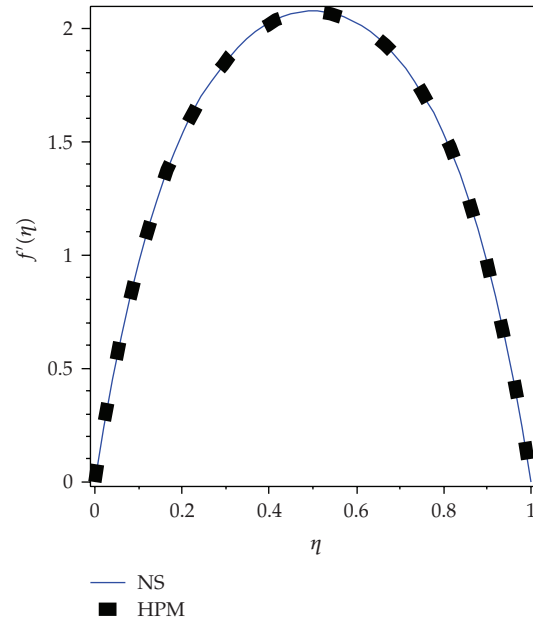


Figure 17: Variation of radial velocity for $M = 5, S = 0.01, A = -1$.

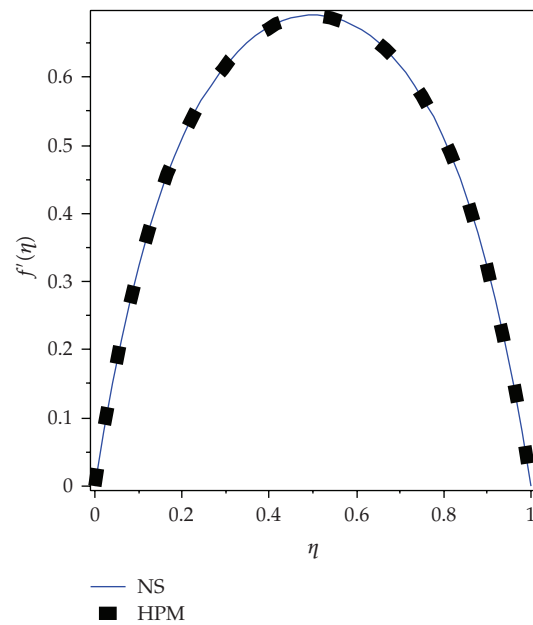


Figure 18: Variation of radial velocity for $M = 5, S = 0.01, A = 0$.

3. Solution Procedure

We consider axisymmetric incompressible flow between two parallel infinite disks, which at time t^* , are spaced a distance $H(1 - at^*)^{1/2}$ apart and a magnetic field proportional to

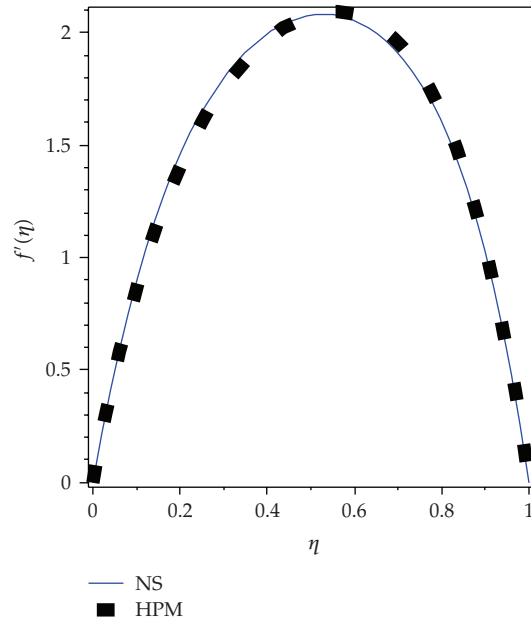


Figure 19: Variation of radial velocity for $M = 5, S = 1, A = -1$.

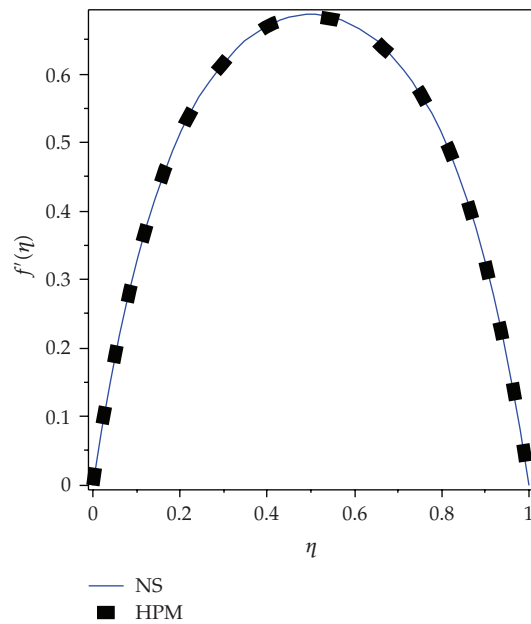


Figure 20: Variation of radial velocity for $M = 5, S = 1, A = 0$.

$B_0(1 - \alpha t^*)^{-1/2}$ is applied perpendicular to the disks. The upper disk at $z = H(1 - \alpha t^*)^{1/2}$ is moving with velocity $-\alpha H(1 - \alpha t^*)^{-1/2}/2$ toward the stationary lower disk at $z = 0$. The axial coordinate is denoted by z^* and the radial coordinate by r^* . With the axial and radial velocities denoted by w^* and u^* , respectively, we introduce the following quantities:

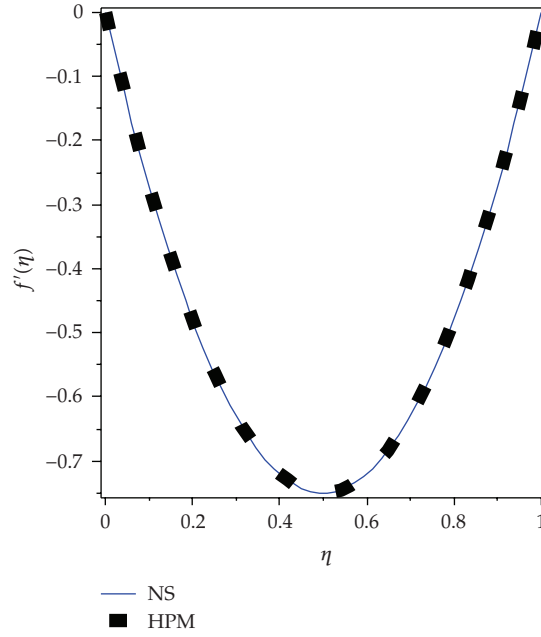


Figure 21: Variation of radial velocity for $M = 0, S = 0.01, A = 1$.

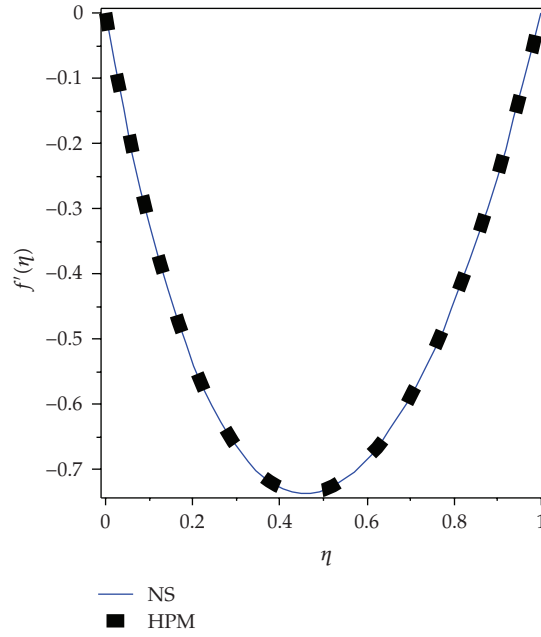


Figure 22: Variation of radial velocity for $M = 0, S = 1, A = 1$.

$$\begin{aligned}
 u^* &= \frac{\alpha r^*}{2(1 - \alpha t^*)} f'(\eta), & w^* &= -\frac{\alpha H}{\sqrt{1 - \alpha t^*}} f(\eta), & B &= \frac{B_0}{\sqrt{1 - \alpha t^*}} \\
 \eta &= \frac{z^*}{H\sqrt{1 - \alpha t^*}}, & r &= r^*, & t &= t^*
 \end{aligned}
 \tag{3.1}$$

into the continuity and momentum equations governing the flow. The continuity equation is automatically satisfied and the momentum equation is reduced to the following fourth-order, nonlinear, ordinary differential equation:

$$f''''(\eta) - S(\eta f'''(\eta) + 3f''(\eta) - 2f(\eta)f'''(\eta)) - M^2 f''(\eta) = 0, \quad (3.2)$$

where primes denote differentiation with respect to the similarity variable η , $(1/r)(\partial p^*/\partial r) = p_1(t)$, $S = (\rho H^2)/2\nu$ and $M = \sigma B_0^2/\mu$. Here ρ denotes the density, μ is the absolute viscosity, ν is kinematic viscosity, σ is the fluid electrical conductivity, B_0 is the magnetic field acting normal to the plates, H is the distance separating the plates at time $t = t^* = 0$ and α a constant and has the units of s^{-1} .

The boundary conditions are given by

$$f(0) = A, \quad f'(0) = 0, \quad f(1) = \frac{1}{2}, \quad f'(1) = 0, \quad (3.3)$$

where A is a constant such that $A > 0$ corresponds to suction and $A < 0$ to injection at the lower stationary disk.

According to the HPM, we can construct a homotopy of (3.2) as follows:

$$H(f, p) = (1 - p)(f'''' - f_0'''') + p(f'''' - S(\eta f''' + 3f'' - 2ff''') - M^2 f''), \quad (3.4)$$

where primes denote differentiation with respect to η and asterisks have been omitted for convenience.

We consider a three term-solution for f as follows:

$$f = f_0 + pf_1 + p^2 f_2. \quad (3.5)$$

Assuming $f_0'''' = 0$ and substituting f from (3.5) into (3.4) and after some algebraic manipulation, we obtain the following set of equations:

$$\begin{aligned} p^0 : f_0'''' &= 0, \\ f_0(0) &= A, \quad f_0'(0) = 0, \quad f_0(1) = 0.5, \quad f_0'(1) = 0 \\ p^1 : -S\eta f_0''' + f_1'''' - 3Sf_0'' + 2Sf_0 f_0''' - M^2 f_0'' &= 0, \\ f_1(0) &= 0, \quad f_1'(0) = 0, \quad f_1(1) = 0, \quad f_1'(1) = 0. \\ p^2 : -M^2 f_1'' - S\eta f_1''' - 3Sf_1'' + 2Sf_1 f_0''' + f_2'''' + 2Sf_0 f_1''' &= 0, \\ f_2(0) &= 0, \quad f_2'(0) = 0, \quad f_2(1) = 0, \quad f_2'(1) = 0. \end{aligned} \quad (3.6)$$

We utilized the symbolic algebra package Maple 11 to solve (3.6) with the appropriate boundary conditions and obtained the following analytical solutions

$$\begin{aligned}
f_0(\eta) &= \frac{1}{6}(-6 + 12A)\eta^3 + \left(\frac{1}{2}(3 - 6A)\eta^2 + A\right), \\
f_1(\eta) &= -3(-1 + 2A)\left(\frac{1}{105}S\eta^7A - \frac{1}{30}S\eta^6A + \frac{1}{6}S\eta^4A - \frac{1}{15}S\eta^5 + \frac{1}{24}M^2\eta^4\right. \\
&\quad \left. + \frac{1}{60}S\eta^6 - \frac{1}{210}S\eta^7 + \frac{1}{8}S\eta^4 - \frac{1}{60}M^2\eta^5\right) \\
&\quad + \frac{1}{6}\left(-\frac{39}{35}SA - \frac{117}{70}S - \frac{3}{5}M^2 + \frac{312}{35}SA^2 + \frac{6}{5}M^2A\right)\eta^3 \\
&\quad + \frac{1}{2}\left(\frac{5}{14}SA + \frac{19}{140}S + \frac{1}{20}M^2 - \frac{44}{35}SA^2 - \frac{1}{10}M^2A\right)\eta^2, \\
f_2(\eta) &= \frac{1}{70}(-1 + 2A)\left(\frac{1}{7920}(1728S^2A^2 - 1728S^2A + 432S^2)\right)\eta^{11} \\
&\quad + \frac{1}{5040}(-604S^2A^2 + 6048S^2A - 1512S^2)\eta^{10} \\
&\quad + \frac{1}{3024}(5040S^2A^2 - 1008M^2SA + 3444S^2 + 504M^2S - 9408S^2A)\eta^9 \\
&\quad + \frac{1}{1680}(2520M^2SA - 1260M^2S + 5040S^2A^2 + 7140S^2A - 4830S^2)\eta^8 \\
&\quad + \frac{1}{840}(70M^4 + 4038S^2 - 9216S^2A^2 + 1498M^2S - 1596M^2SA - 108S^2A)\eta^7 \quad (3.7) \\
&\quad + \frac{1}{360}(-105M^4 - 546M^2SA - 4164S^2A + 2400S^2A^2 - 987M^2S - 1983S^2)\eta^6 \\
&\quad + \frac{1}{120}(1680S^2A^2 + 468S^2 + 732M^2SA + 285M^2S + 2508S^2A + 42M^4)\eta^5 \\
&\quad + \frac{1}{24}\left(-\frac{624}{35}S^2A^3 - \frac{128}{35}M^2SA^2 + \frac{44}{35}M^2SA - \frac{1}{10}M^4A + \frac{2}{7}M^2S - \frac{54}{35}S^2A^2\right. \\
&\quad \left. + \frac{57}{140}S^2 + \frac{309}{70}S^2A + \frac{1}{20}M^4\right)\eta^4 \\
&\quad + \frac{1}{6}\left(-\frac{17}{140}M^2SA + \frac{9}{1400}M^2S - \frac{32773}{40425}S^2A^2 + \frac{779}{64680}S^2 - \frac{50339}{161700}S^2A\right. \\
&\quad \left. + \frac{38}{175}M^2SA^2 + \frac{7466}{2695}S^2A^3 + \frac{1}{1400}M^4 - \frac{1}{700}M^4A\right)\eta^3 \\
&\quad + \frac{1}{2}\left(-\frac{1}{525}M^2SA + \frac{5414}{40425}S^2A^2 - \frac{2047}{646800}S^2 - \frac{3253}{323400}S^2A - \frac{1}{2800}M^4\right. \\
&\quad \left. + \frac{13}{1050}M^2SA^2 - \frac{2726}{13475}S^2A^3 + \frac{1}{1400}M^4A - \frac{3}{1400}M^2S\right)\eta^2, \\
f(\eta) &= f_0(\eta) + f_1(\eta) + f_2(\eta).
\end{aligned}$$

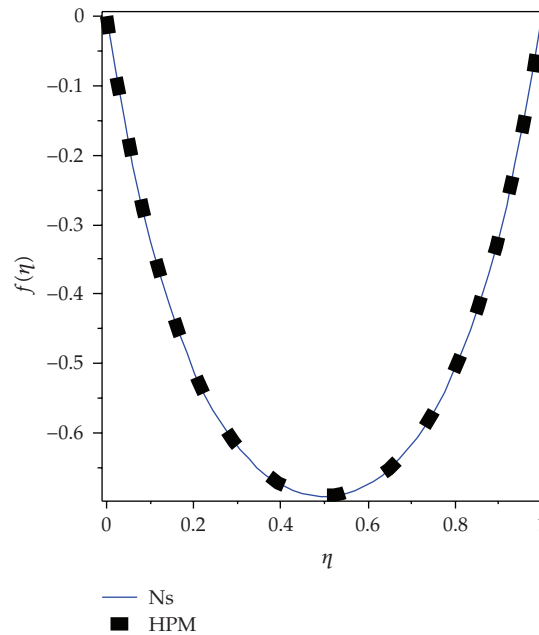


Figure 23: Variation of radial velocity for $M = 5$, $S = 0.01$, $A = 1$.

Once $f(\eta)$ is known in an analytical form, the definition of u^* in (3.1) can be used to calculate the axial component of the velocity, u^* . By differentiating $f(\eta)$ with respect to η , which is straightforward and can be easily performed by Maple 11, we use the definition of w^* in (3.1) to compute the radial component of the velocity.

The axial and radial velocities are each functions of parameters S , M and A . Since the axial and radial velocities are proportional to f and f' , respectively, they suffice to present the results for f . These results are displayed in Figures 1, 2, 3, 4, 5, 6, 7, 8, 9, 10, 11, and 12 for twelve different combinations of parameters S , M , and A . Figures 1–8 show that for both the cases of no injection ($A = 0$) and injection ($A < 0$), the axial component of the velocity increases monotonically as η increases. The velocity profile is not significantly affected by the increase in the fluid electrical conductivity and/or the magnetic field, that is, the increase in M from 0 to 5. A careful examination of Figures 1–8 also reveals that the effect of squeeze Reynolds number S on the axial velocity profiles is minimal.

Figures 9–12 show the effect of suction ($A > 0$) on the axial velocity distributions. In each case, the axial velocity decreases monotonically as η increases. Siddiqui et al. [20] have observed the same pattern for the axial (normal in their case) velocity in the study of two-dimensional MHD squeeze flow between parallel plates without injection or suction. As in the case for injection (Figures 1–8), the velocity patterns are only minimally influenced by the changes in parameters M and S .

The results for f' which represents the radial component of the velocity appear in Figures 13, 14, 15, 16, 17, 18, 19, 20, 21, 22, 23, and 24. Figures 13–20 show the results for the radial velocity with no injection ($A = 0$) and injection ($A < 0$) for different combination values of M and S . In each case, the radial velocity increases as η increases, reaches a peak value in the neighborhood of $\eta = 0.5$ and then decays to zero around $\eta = 1$. For the case of suction ($A > 0$), which is illustrated in Figures 21–24, the radial velocity becomes negative

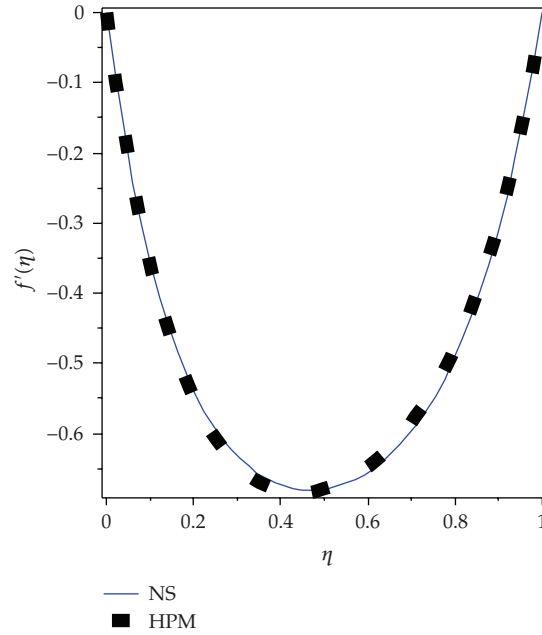


Figure 24: Variation of radial velocity for $M = 5$, $S = 1$, $A = 1$.

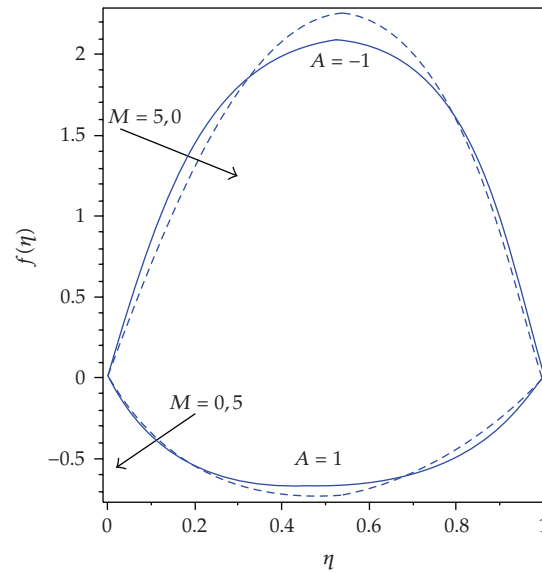


Figure 25: Variation of radial velocity with M and A for $S = 1$.

and decreases as η increases. The trough in radial velocity is attained in the neighborhood of $\eta = 0.5$. After that the velocity increases and reaches the zero value around $\eta = 1$.

Figure 25 has been prepared to illustrate the effect of varying the imposed magnetic field (Hartmann number M) on the radial distribution of velocity for suction ($A = 1$) and injection ($A = -1$). As the strength of the magnetic field is increased, that is, as the

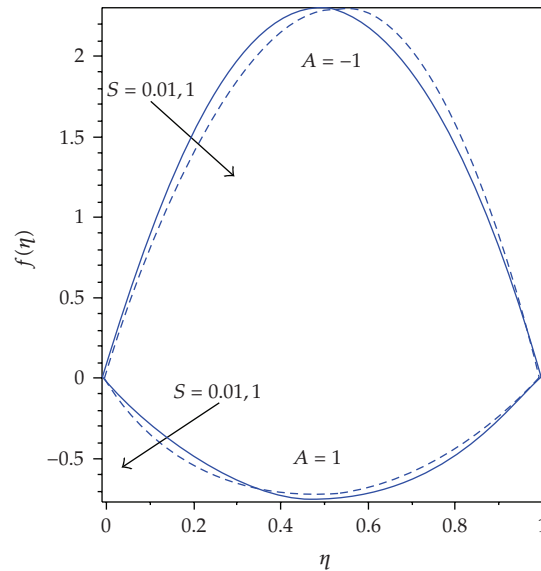


Figure 26: Variation of radial velocity with S and A for $M = 5$.

Hartmann number increases, the impact is felt most on the maximum radial velocity, more so for injection than for suction. The effect of squeeze Reynolds number S on the radial velocity distribution is shown in Figure 26 for a fixed value of $M = 5$. It can be seen that even with a hundred-fold increase in S , the radial velocity profile is not affected significantly.

For every case investigated (Figures 1–26), the HPM predictions have been compared with the corresponding direct numerical solutions (NSs) obtained by using Maple 11 software. This software uses a Fehlberg fourth-fifth order Runge-Kutta finite-difference method for the numerical solution of the boundary value problem [34]. In each case, the HPM and NS are found to be consistently close. This consistent closeness strongly vouches for the accuracy of HPM. Equation (3.7) therefore provides simple and highly accurate analytical solutions for the problem studied in this paper and is useful for rapid engineering calculations.

4. Conclusions

He's homotopy perturbation method (HPM) has been utilized to derive approximate analytical solutions for the radial and axial velocity distributions in magneto-hydrodynamic (MHD) squeeze flow between two parallel infinite disks where one disk is impermeable and the other is porous with either suction or injection of the fluid. The approximate solutions have been compared with the direct numerical solutions generated by the symbolic algebra package Maple 11 which uses a Fehlberg fourth-fifth order Runge-Kutta finite-difference method for solving nonlinear boundary value problems. The comparison showed that the HPM solutions are highly accurate and provide a rapid means of computing the flow velocities between the plates.

For both the cases of no injection and injection, the axial component of the velocity increases monotonically as the similarity variable increases. The velocity profiles are not

significantly affected by the increase in the fluid electrical conductivity and/or the magnetic field. Similarly, the effect of squeeze Reynolds number S on the axial velocity profiles is minimal. The effect of imposed magnetic field on the maximum radial velocity is more pronounced for injection than for suction.

Acknowledgment

The authors express their gratitude to the reviewers for their valuable suggestions which were incorporated to enhance the value of the paper.

References

- [1] W. F. Hughes and R. A. Elco, "Magnetohydrodynamic lubrication flow between parallel rotating disks," *Journal of Fluid Mechanics*, vol. 13, no. 1, pp. 21–32, 1962.
- [2] D. C. Kuzma, E. R. Maki, and R. J. Donnelly, "The magnetohydrodynamic squeeze film," *Journal of Fluid Mechanics*, vol. 19, no. 3, pp. 395–400, 1964.
- [3] R. J. Krieger, H. J. Day, and W. F. Hughes, "The MHD hydrostatics thrust bearings—theory and experiments," *ASME Journal of Lubrication Technology*, vol. 89, pp. 307–313, 1967.
- [4] J.-H. He, "Homotopy perturbation technique," *Computer Methods in Applied Mechanics and Engineering*, vol. 178, no. 3-4, pp. 257–262, 1999.
- [5] J.-H. He, "Approximate analytical solution for seepage flow with fractional derivatives in porous media," *Computer Methods in Applied Mechanics and Engineering*, vol. 167, no. 1-2, pp. 57–68, 1998.
- [6] J.-H. He, "A review on some new recently developed nonlinear analytical techniques," *International Journal of Nonlinear Sciences and Numerical Simulation*, vol. 1, no. 1, pp. 51–70, 2000.
- [7] D. D. Ganji and A. Rajabi, "Assessment of homotopy-perturbation and perturbation methods in heat radiation equations," *International Communications in Heat and Mass Transfer*, vol. 33, no. 3, pp. 391–400, 2006.
- [8] D. D. Ganji and A. Sadighi, "Application of He's homotopy-perturbation method to nonlinear coupled systems of reaction-diffusion equations," *International Journal of Nonlinear Sciences and Numerical Simulation*, vol. 7, no. 4, pp. 411–418, 2006.
- [9] P. D. Ariel, T. Hayat, and S. Asghar, "Homotopy perturbation method and axisymmetric flow over a stretching sheet," *International Journal of Nonlinear Sciences and Numerical Simulation*, vol. 7, no. 4, pp. 399–406, 2006.
- [10] S. H. Hosein Nia, A. N. Ranjbar, D. D. Ganji, H. Soltani, and J. Ghasemi, "Maintaining the stability of nonlinear differential equations by the enhancement of HPM," *Physics Letters A*, vol. 372, no. 16, pp. 2855–2861, 2008.
- [11] T. Öziş and A. Yıldırım, "Comparison between Adomian's method and He's homotopy perturbation method," *Computers & Mathematics with Applications*, vol. 56, no. 5, pp. 1216–1224, 2008.
- [12] A. Beléndez, T. Beléndez, A. Márquez, and C. Neipp, "Application of He's homotopy perturbation method to conservative truly nonlinear oscillators," *Chaos, Solitons & Fractals*, vol. 37, no. 3, pp. 770–780, 2008.
- [13] X. Ma, L. Wei, and Z. Guo, "He's homotopy perturbation method to periodic solutions of nonlinear Jerk equations," *Journal of Sound and Vibration*, vol. 314, no. 1-2, pp. 217–227, 2008.
- [14] A. M. Siddiqui, A. Zeb, Q. K. Ghorri, and A. M. Benharbit, "Homotopy perturbation method for heat transfer flow of a third grade fluid between parallel plates," *Chaos, Solitons & Fractals*, vol. 36, no. 1, pp. 182–192, 2008.
- [15] B. G. Zhang, S. Y. Li, and Z. R. Liu, "Homotopy perturbation method for modified Camassa-Holm and Degasperis-Procesi equations," *Physics Letters A*, vol. 372, no. 11, pp. 1867–1872, 2008.
- [16] L.-N. Zhang and J.-H. He, "Homotopy perturbation method for the solution of the electrostatic potential differential equation," *Mathematical Problems in Engineering*, vol. 2006, Article ID 83878, 6 pages, 2006.
- [17] M. Rafei, H. Daniali, D. D. Ganji, and H. Pashaei, "Solution of the prey and predator problem by homotopy perturbation method," *Applied Mathematics and Computation*, vol. 188, no. 2, pp. 1419–1425, 2007.

- [18] D. D. Ganji and A. Sadighi, "Application of homotopy-perturbation and variational iteration methods to nonlinear heat transfer and porous media equations," *Journal of Computational and Applied Mathematics*, vol. 207, no. 1, pp. 24–34, 2007.
- [19] M. Esmailpour and D. D. Ganji, "Application of He's homotopy perturbation method to boundary layer flow and convection heat transfer over a flat plate," *Physics Letters A*, vol. 372, no. 1, pp. 33–38, 2007.
- [20] A. M. Siddiqui, S. Irum, and A. R. Ansari, "Unsteady squeezing flow of a viscous MHD fluid between parallel plates, a solution using the homotopy perturbation method," *Mathematical Modelling and Analysis*, vol. 13, no. 4, pp. 565–576, 2008.
- [21] J.-H. He, "An elementary introduction to the homotopy perturbation method," *Computers & Mathematics with Applications*, vol. 57, no. 3, pp. 410–412, 2009.
- [22] J.-H. He, "An elementary introduction to recently developed asymptotic methods and nanomechanics in textile engineering," *International Journal of Modern Physics B*, vol. 22, no. 21, pp. 3487–3578, 2008.
- [23] J.-H. He, "Recent development of the homotopy perturbation method," *Topological Methods in Nonlinear Analysis*, vol. 31, no. 2, pp. 205–209, 2008.
- [24] A. Yıldırım, "Homotopy perturbation method to obtain exact special solutions with solitary patterns for Boussinesq-like $B(m, n)$ equations with fully nonlinear dispersion," *Journal of Mathematical Physics*, vol. 50, no. 2, Article ID 023510, 10 pages, 2009.
- [25] A. Yıldırım, "An algorithm for solving the fractional nonlinear Schrödinger equation by means of the homotopy perturbation method," *International Journal of Nonlinear Sciences and Numerical Simulation*, vol. 10, no. 4, pp. 445–451, 2009.
- [26] A. Yıldırım, "Application of He's homotopy perturbation method for solving the Cauchy reaction-diffusion problem," *Computers & Mathematics with Applications*, vol. 57, no. 4, pp. 612–618, 2009.
- [27] A. Yıldırım, "The homotopy perturbation method for solving the modified Korteweg-de Vries equation," *Zeitschrift für Naturforschung A*, vol. 63a, no. 10-11, pp. 621–626, 2008.
- [28] A. Yıldırım, "Solution of BVPs for fourth-order integro-differential equations by using homotopy perturbation method," *Computers & Mathematics with Applications*, vol. 56, no. 12, pp. 3175–3180, 2008.
- [29] A. Yıldırım, "Exact solutions of nonlinear differential-difference equations by He's homotopy perturbation method," *International Journal of Nonlinear Sciences and Numerical Simulation*, vol. 9, no. 2, pp. 111–114, 2008.
- [30] A. Yıldırım and T. Öziş, "Solutions of singular IVPs of Lane-Emden type by homotopy perturbation method," *Physics Letters A*, vol. 369, no. 1-2, pp. 70–76, 2007.
- [31] M. Mahmood, M. A. Hossain, S. Asghar, and T. Hayat, "Application of homotopy perturbation method to deformable channel with wall suction and injection in a porous medium," *International Journal of Nonlinear Sciences and Numerical Simulation*, vol. 9, no. 2, pp. 195–206, 2008.
- [32] A. A. Mehmood and A. Ali, "An application of He's homotopy perturbation method in fluid mechanics," *International Journal of Nonlinear Sciences and Numerical Simulations*, vol. 10, no. 2, pp. 239–246, 2009.
- [33] Z. Z. Ganji and D. D. Ganji, "Approximate solutions of thermal boundary-layer problems in a semi-infinite flat plate by using He's homotopy perturbation method," *International Journal of Nonlinear Sciences and Numerical Simulation*, vol. 9, no. 4, pp. 415–422, 2008.
- [34] A. Heck, *Introduction to Maple*, Springer, New York, NY, USA, 2nd edition, 1996.